



Contents lists available at ScienceDirect

Tectonophysics

journal homepage: www.elsevier.com/locate/tecto

The April 2007 earthquake swarm near Lake Trichonis and implications for active tectonics in western Greece

A. Kiratzi^{a,*}, E. Sokos^b, A. Ganas^c, A. Tselentis^b, C. Benetatos^a, Z. Roumelioti^a, A. Serpetzidaki^b, G. Andriopoulos^b, O. Galanis^a, P. Petrou^c

^a Department of Geophysics, Aristotle University of Thessaloniki, 54124 Thessaloniki, Greece

^b Seismological Laboratory, University of Patras, Rio 261 10, Greece

^c National Observatory of Athens, Geodynamic Institute, 11810 Athens, Greece

ARTICLE INFO

Article history:

Received 18 September 2007

Received in revised form 4 February 2008

Accepted 14 February 2008

Available online xxx

Keywords:

Lake Trichonis

Western Greece

Focal mechanisms

Strike-slip

Earthquake

Tectonics

ABSTRACT

We investigate the properties of the April 2007 earthquake swarm (Mw 5.2) which occurred at the vicinity of Lake Trichonis (western Greece). First we relocated the earthquakes, using P- and S-wave arrivals to the stations of the Hellenic Unified Seismic Network (HUSN), and then we applied moment tensor inversion to regional broad-band waveforms to obtain the focal mechanisms of the strongest events of the 2007 swarm. The relocated epicentres, cluster along the eastern banks of the lake, and follow a distinct NNW–ESE trend. The previous strong sequence close to Lake Trichonis occurred in June–December 1975. We applied teleseismic body waveform inversion, to obtain the focal mechanism solution of the strongest earthquake of this sequence, e.g. the 31 December 1975 (Mw 6.0) event. Our results indicate that: a) the 31 December 1975 Mw 6.0 event was produced by a NW–SE normal fault, dipping to the NE, with considerable sinistral strike-slip component; we relocated its epicentre: i) using phase data reported to ISC and its coordinates are 38.486°N, 21.661°E; ii) using the available macroseismic data, and the coordinates of the macroseismic epicentre are 38.49°N, 21.63°E, close to the strongly affected village of Kato Makrinou; b) the earthquakes of the 2007 swarm indicate a NNW–SSE strike for the activated main structure, parallel to the eastern banks of Lake Trichonis, dipping to the NE and characterized by mainly normal faulting, occasionally combined with sinistral strike-slip component. The 2007 earthquake swarm did not rupture the well documented E–W striking Trichonis normal fault that bounds the southern flank of the lake, but on the contrary it is due to rupture of a NW–SE normal fault that strikes at a ~45° angle to the Trichonis fault. The left-lateral component of faulting is mapped for the first time to the north of the Gulf of Patras which was previously regarded as the boundary for strike-slip motions in western Greece. This result signifies the importance of further investigations to unravel in detail the tectonics of this region.

© 2008 Elsevier B.V. All rights reserved.

1. Introduction

On 8 April 2007 an earthquake swarm burst near the SE bank of Lake Trichonis, a lake overlying the Trichonis graben in western Greece. The three strongest events of the swarm occurred on April 10th at 03:17, 07:15 and 10:41 GMT with moderate magnitudes ranging from Mw 5.0 to Mw 5.2. The most serious damage was reported in the village Thermon 5 km to the NE of the earthquake epicentres. Lake Trichonis, located to the east of the city of Agrinio and to the north of the cities of Nafpaktos and Messolongi, is the largest natural lake in Greece, with surface area of 97 km², a maximum water depth of 58 m and an approximate water volume of 2.8 × 10⁹ m³ (Zacharias et al., 2005). The lake itself constitutes a significant ecosystem.

Fig. 1 summarizes the historical (before 1911 for Greece) and instrumental seismicity with Mw ≥ 6.0, together with the Mw ≥ 4.0

seismicity as relocated by Roumelioti et al. (2007), and the focal mechanisms of the strongest previous events from the database of Kiratzi and Louvari (2003) and Kiratzi et al. (in press). It is clearly seen that Lake Trichonis and its immediate vicinity have never been the site of frequent strong earthquakes (Ambraseys, 2001a,b; Papazachos and Papazachou, 2003). The seismicity is sparse and the strongest event registered for the region occurred in 1975. However by looking closely, a concentration of epicentres around the south-east area of Lake Trichonis is observed. In the past, the city of Agrinio, at the northwestern bank of the lake, was severely affected by the occurrence of an intermediate depth event (not shown in Fig. 1) on 31 March 1965 (GMT 09:47:31, 38.6°N, 22.4°E, $h=78$ km, $M=6.8$, $Io=VIII+$ in Agrinio), whereas the city of Nafpaktos was mostly affected by the 24 December 1917 event (GMT 09:13:55; 38.4°N, 21.7°E; $h=n$, $M=6.0$, $Io=VIII$ in Nafpaktos; Papazachos and Papazachou, 2003).

In this study, we first revisit the strongest 1975 events, in order to relocate them, invert for the focal mechanism using teleseismic recordings and search for evidence for the fault plane; then, we study the 2007 swarm using regional digital broad-band records to calculate

* Corresponding author. Tel.: +30 2310 998486; fax: +30 2310 998528.
E-mail address: Kiratzi@geo.auth.gr (A. Kiratzi).



Table 1
Parameters (here determined or previously published) for the 30 June and 31 December 1975 events

Year	Month	Day	h:min:s	Lat °N	Lon °E	Depth km	Mw	Nodal plane 1			Nodal plane 2			P axis		T axis		Reference	
								Strike °	Dip °	Rake °	Strike °	Dip °	Rake °	az °	pl °	az °	pl °		
1975	06	30	13:26:55.3	38.466	21.641	4.4	5.6												This work – epicentre relocated with Hypoinverse using ISC phases This work – parameters determined using macroseismic data National Observatory of Athens (NOA) bulletins NEIS ISC Macroseismic epicentre (Papazachos et al., 1997)
				38.481	21.671	–	5.6±0.17	112°±16° (or 292°)											
				38.4	21.7	–	5.4 Ms												
				38.539	21.645	11	5.4 ML												
				38.489	21.623	3.1	5.0 mb												
				38.48	21.63	–	5.7												
1975	12	21	16:07:52.40	38.42	21.71	–	5.5	352	46	–54	126	54	–121	337	65	238	4	Focal mechanism with P-wave first motions (SP data) (Delibasis and Carydis, 1977)	
1975	12	31	09:45:45.55	38.486	21.661	4+2/-2	6.0	316+5/-10	71+10/-20	–26+10/-10	55	66	–159	274	31	6	3	This work – epicentre relocated with Hypoinverse – depth and mechanism from teleseismic waveform modelling	
				38.489	21.632	–	5.9±0.14	137°±34° (or 317°)	n/a									This work – parameters determined using macroseismic data National Observatory of Athens (NOA) bulletins and Papazachos (1975)	
				38.5	21.7	–	5.9 Ms	236	39	–125	98	59	–65	55	66	170	11	NEIS ISC	
				38.63	21.80	19	5.5 Ms											Macroseismic epicentre (Papazachos et al., 1997)	
				38.524	21.673	15	5.5 Ms												
				38.51	21.61	9	5.7												



31 December 1975Moment: 1.13×10^{18} Ntm ~ **Mw 6.0**

Depth: 4 km

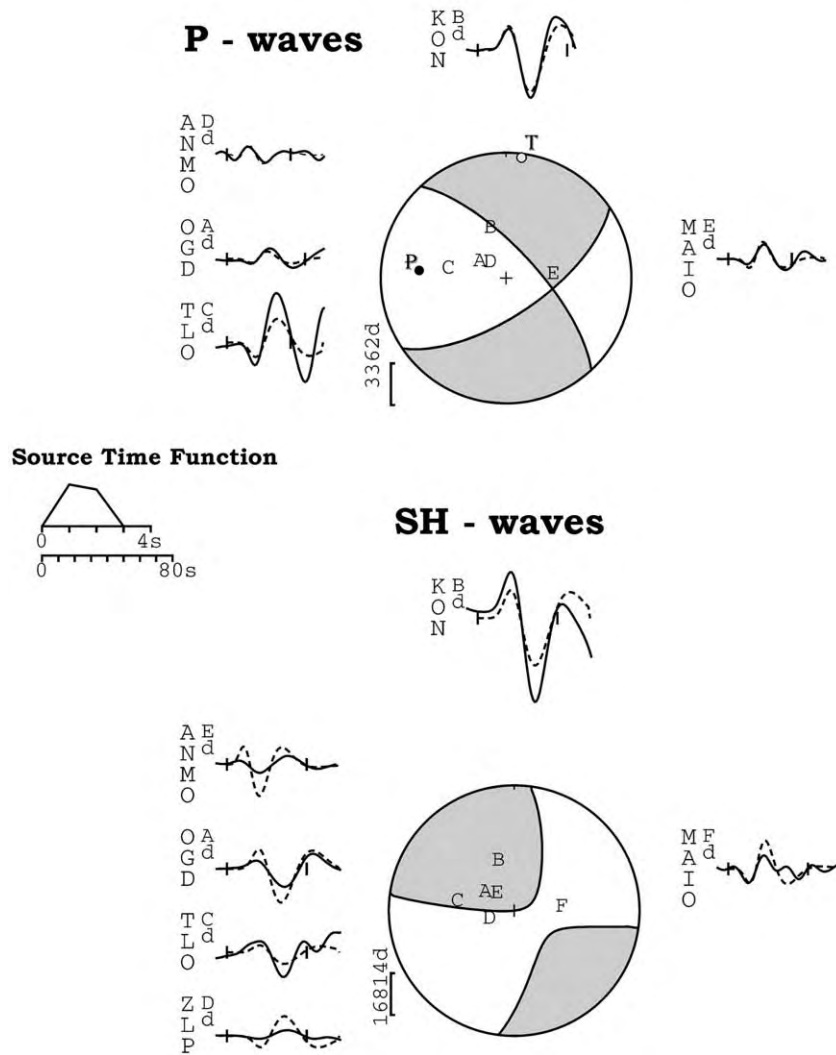


Fig. 2. Minimum misfit solution for the 31 December 1975 (the strongest instrumentally recorded event close to the 2007 swarm) calculated by inverting P and SH body waves for a point source, in a half-space of $V_p=6.5$ km/s, $V_s=3.7$ km/s and $\rho=2.8$ g/cm³. The focal spheres show P (top) and SH (bottom) nodal planes in lower hemisphere projections; Observed (solid) and synthetic (dashed) waveforms are plotted around the focal spheres; the inversion window is indicated by vertical ticks, station codes are written vertically and station positions denoted by capital letters. The STF is the source time function, and the scale bar below it (in s) is that of the waveforms. P and T axes are also marked.

the west, and its flow is reversed, as it now flows to the north. It is therefore reasonable to assume that it is the late Quaternary footwall uplift of the Trichonis fault that has affected the whole process.

It is generally observed that during the 6 month period of April to September, 40% of the total annual outflows of the Trichonis Lake are pumped for agricultural purposes which results in very rapid water level drops more than 60 cm (mainly May–September) causing extended drought in the wetland area (Zacharias et al., 2005). It is of interesting to note that both, the 1975 sequence and the 2007 swarm occurred within this period, but this is mainly a qualitative observation at this point.

3. The June–December 1975 sequence

3.1. Teleseismic waveform modelling of the 31 December 1975 event

The June–December 1975 seismic sequence is the most recent instrumentally recorded near the southern flank of Lake Trichonis.

Two were the strongest events of the sequence, (Table 1 for parameters) which occurred on 30 June (Mw 5.6) and 31 December 1975 (Mw 6.0). The last event was preceded on 21 December 1975 by another strong (Mw 5.5) event, which occurred farther to the south of the activated region (Fig. 5). It was the 31 December event that produced landslides (Papadopoulos and Plessa, 2000) considerable structural damage at Kato Makrinou (200 old houses destroyed and 580 seriously cracked); one death and two injuries (Io=VIII–IX at Kato Makrinou; National Observatory of Athens (NOA) bulletins).

The focal mechanisms of the two strongest events of the region are significant for this study and the search at the IRIS depository for both events provided a number of good signal/noise waveforms for only the 31 December 1975 event. The 30 June 1975 event, had noisy records, and a teleseismic focal mechanism determination was not possible. A first motion polarity solution was not feasible either, due to insufficient data reported at IRIS.

For the 31 December 1975 event we retrieved 5 P and 6 SH waveforms with good signal/noise ratio from stations in teleseismic (30°

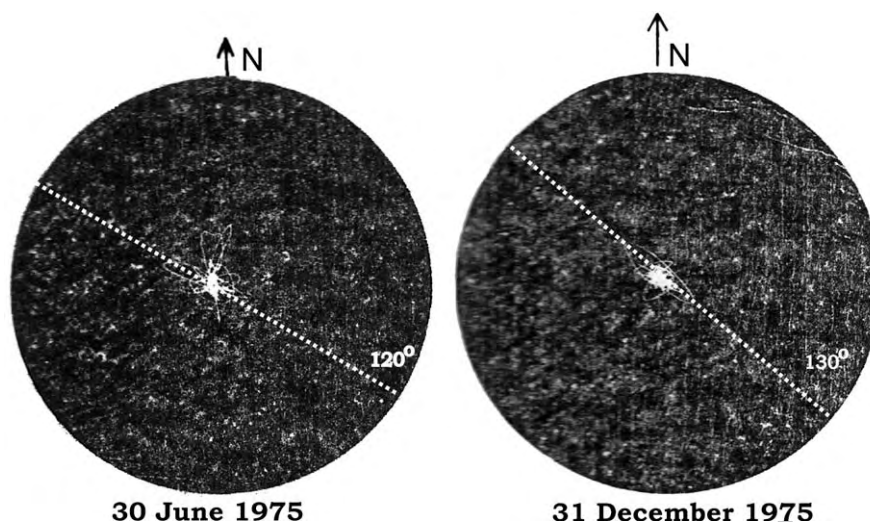


Fig. 3. Seismoscope (SR-100 Wilmot) records for the 30 June 1975 (left) and the 31 December 1975 (right) events obtained at Messolongi (Fig. 1 for location) ~24 km to the SW of the June–December 1975 epicentres. The records shown are those as included in the National Observatory of Athens (NOA) monthly bulletins. The 30 June 1975 caused a deflection of 13.6 mm in the N120°E direction and the 31 December 1975 event caused a deflection of 13.5 mm at ~N130°E (Person, 1977).

151 to 90° distances. We used the MT5 software (Zwick et al., 1994) and the
 152 analysis procedures as described in detail elsewhere (e.g. Kiratzi and
 Q2 153 Louvari, 2001; Benetatos et al., 2004, 2005 and references therein) to
 154 invert for the focal mechanism parameters (strike/dip/rake), centroid
 155 depth and seismic moment, assuming a source represented as a point in
 156 space and described in time by a source time function consisting of
 157 overlapping isosceles triangles. Prior to the inversion waveforms have
 158 been filtered between 0.01 and 0.1 Hz and convolved with a typical

WWSSN 15–100 s long-period instrument response. Green's functions
 159 have been calculated using a half-space of 6.5 km/s and 3.7 km/s for
 160 P-waves and S-waves, respectively and a density of 2.8 g/cm³. 161

The best fitting solution (known as “the minimum misfit solution”),
 162 obtained after many test inversions, (Table 1 and Fig. 2) indicates normal
 163 faulting with a considerable strike-slip component. The simple-shape
 164 source time function has a total duration of 3 s. The solution obtained
 165 from waveform modelling, is in accordance with the mechanism
 166

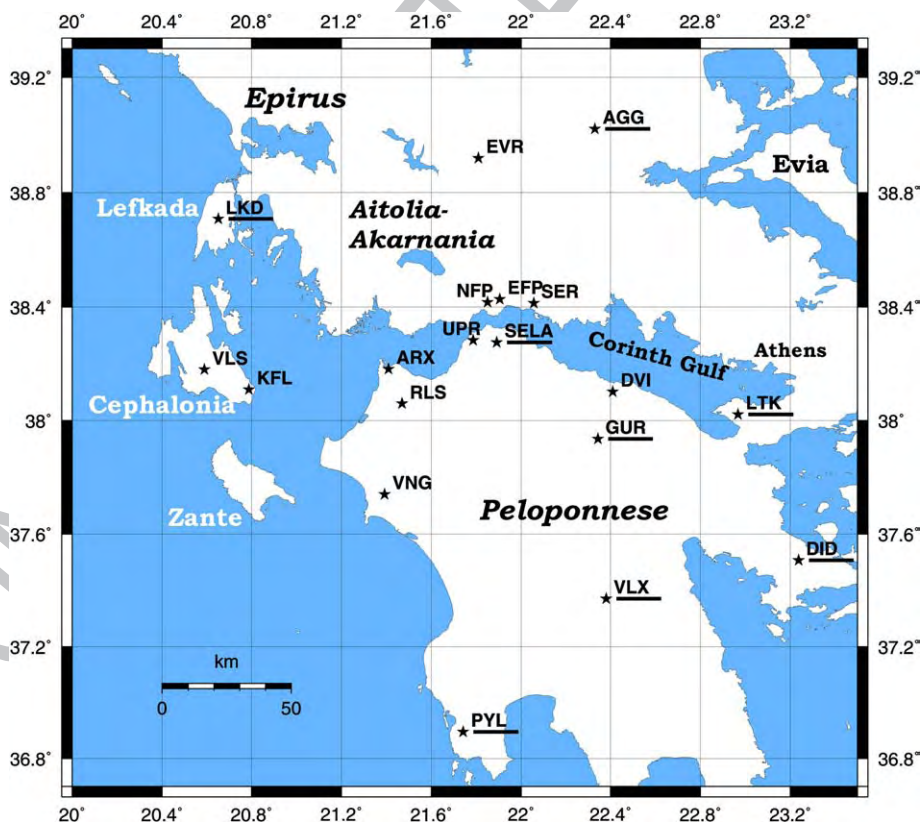


Fig. 4. Location of the broad-band stations (stars) of the Hellenic Unified Seismograph Network (HUSN), whose records were used in the relocation of epicentres (all stations were used) and the focal mechanism determination (station names underlined).

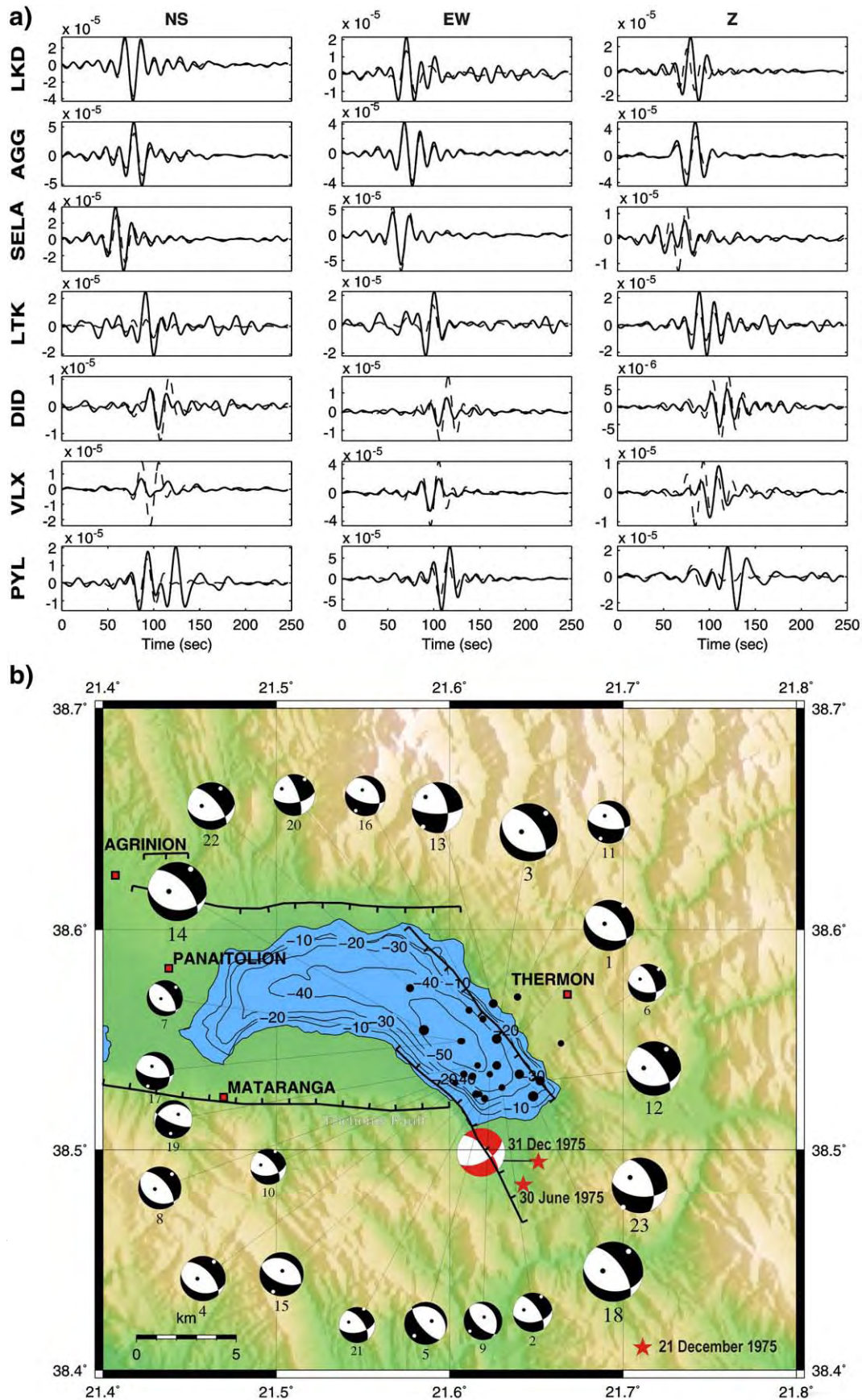


Fig. 5. a) Waveform fit between observed (solid line) and synthetic waveforms (dashed line) for event no. 14 in Table 2. Displacement waveforms are presented and amplitude scale is in meters. b) Focal mechanisms for twenty-three events of the 2007 swarm determined using regional moment tensor inversion (see Table 2 for parameters). Normal faulting along NNW–SSE trending planes is observed combined with strike-slip motions, for two events of the sequence pure strike-slip motions are observed. The 1975 epicentres and the mechanism for the 31 December 1975 event are included for comparison.

t2.1 **Table 2**

Source parameters for the strongest 2007 events determined from regional moment tensor inversion (ISOLA code – see text for details); Q = quality of the solution based on the % of variance reduction, VR, with thresholds set at VR < 40%, 60% < VR < 40%, VR > 60% for Q = C, B, A respectively; DC = double-couple percentage, CLVD = compensated linear vector dipole percentage; all locations are obtained by HypoDD except for events 18, and 23 which were obtained from Hypoinverse

No.	Year	Month	Day	h:min:s	Lat °N	Lon °E	Depth km	Mw	Nodal plane 1			Nodal plane 2			P axis		T axis		Q	CLVD %	VR %	
									Strike °	Dip °	Rake °	Strike °	Dip °	Rake °	az °	pl °	az °	pl °				
t2.5	1	2007	4	09	23:27:15.71	38.539	21.626	15.66	4.4	320	51	-71	111	43	-112	291	75	36	4	A	55	70
t2.6	2	2007	4	10	00:54:56.35	38.529	21.629	14.91	3.4	327	65	-48	82	48	-145	286	51	28	10	B	5	48
t2.7	3	2007	4	10	03:17:56.09	38.551	21.626	14.29	5.0	325	59	-72	113	35	-117	274	70	42	12	A	26	74
t2.8	4	2007	4	10	03:27:38.33	38.534	21.612	5.28	3.9	317	59	-71	103	36	-119	269	70	33	12	C	13	38
t2.9	5	2007	4	10	03:32:34.20	38.524	21.619	14.15	3.7	296	24	-112	140	68	-80	67	66	223	22	A	51	64
t2.10	6	2007	4	10	03:39:18.86	38.549	21.663	12.49	3.3	337	61	-50	97	48	-139	299	55	40	7	C	24	31
t2.11	7	2007	4	10	04:16:15.65	38.550	21.605	2.95	3.1	324	60	-78	121	32	-110	263	72	45	14	C	42	20
t2.12	8	2007	4	10	04:29:58.11	38.535	21.607	10.96	3.7	320	61	-78	116	31	-111	257	71	41	15	A	23	62
t2.13	9	2007	4	10	04:47:17.99	38.535	21.622	12.94	3.3	336	32	-71	134	60	-101	16	73	232	14	C	20	27
t2.14	10	2007	4	10	05:55:12.15	38.531	21.602	9.70	3.1	322	61	-49	81	49	-140	284	54	24	7	B	20	51
t2.15	11	2007	4	10	06:03:39.12	38.570	21.638	8.54	3.7	327	37	-47	98	64	-117	326	61	207	15	B	5	53
t2.16	12	2007	4	10	07:13:03.67	38.532	21.651	14.60	4.7	323	66	-63	92	36	-135	273	60	33	16	A	38	70
t2.17	13	2007	4	10	07:14:12.39	38.567	21.624	12.42	4.4	348	59	-23	90	70	-147	312	37	217	7	A	36	66
t2.18	14	2007	4	10	07:15:40.44	38.555	21.584	5.06	5.1	317	60	-67	97	37	-124	271	67	31	12	B	28	56
t2.19	15	2007	4	10	08:13:45.40	38.526	21.614	14.59	3.8	300	32	-84	113	58	-94	12	77	206	13	A	15	61
t2.20	16	2007	4	10	09:59:01.51	38.560	21.618	11.63	3.5	331	37	-50	105	63	-116	333	63	213	14	B	36	57
t2.21	17	2007	4	10	10:34:47.97	38.550	21.606	13.62	3.3	320	35	-55	99	62	-112	329	66	205	14	A	53	63
t2.22	18	2007	4	10	10:41:00.14	38.525	21.647	22.47	5.2	325	64	-65	98	35	-131	275	62	37	16	A	31	65
t2.23	19	2007	4	10	12:55:17.70	38.539	21.615	12.91	3.3	247	24	-133	113	73	-73	46	59	190	26	C	5	36
t2.24	20	2007	4	10	13:51:00.93	38.564	21.610	17.81	3.6	341	74	-32	81	59	-161	297	34	34	10	C	9	38
t2.25	21	2007	4	13	12:58:14.45	38.526	21.616	9.38	3.1	325	60	-42	79	55	-142	290	49	23	3	C	3	38
t2.26	22	2007	4	15	02:16:32.58	38.574	21.576	17.86	4.1	320	67	-60	84	37	-140	271	57	28	17	A	48	69
t2.27	23	2007	6	5	11:50:20.46	38.535	21.639	16.57	4.8	339	54	-42	97	57	-136	310	53	217	2	B	23	50
t2.28	2007 swarm average focal mechanism									325	52	-58	99	48	-124	298	65	33	2			

167 reported in Delibasis and Carydis (1977). It differs from the composite
 168 solution, obtained from first motion polarities of short-period records
 169 (Papazachos, 1975), which showed almost pure E–W normal faulting

(NP1: strike=98°, dip=59°, rake=-65°, NP2: strike=236°, dip=39°, rake=-125°). To test the validity of a pure normal mechanism we did forward modelling by keeping the focal parameters (strike, dip and rake)

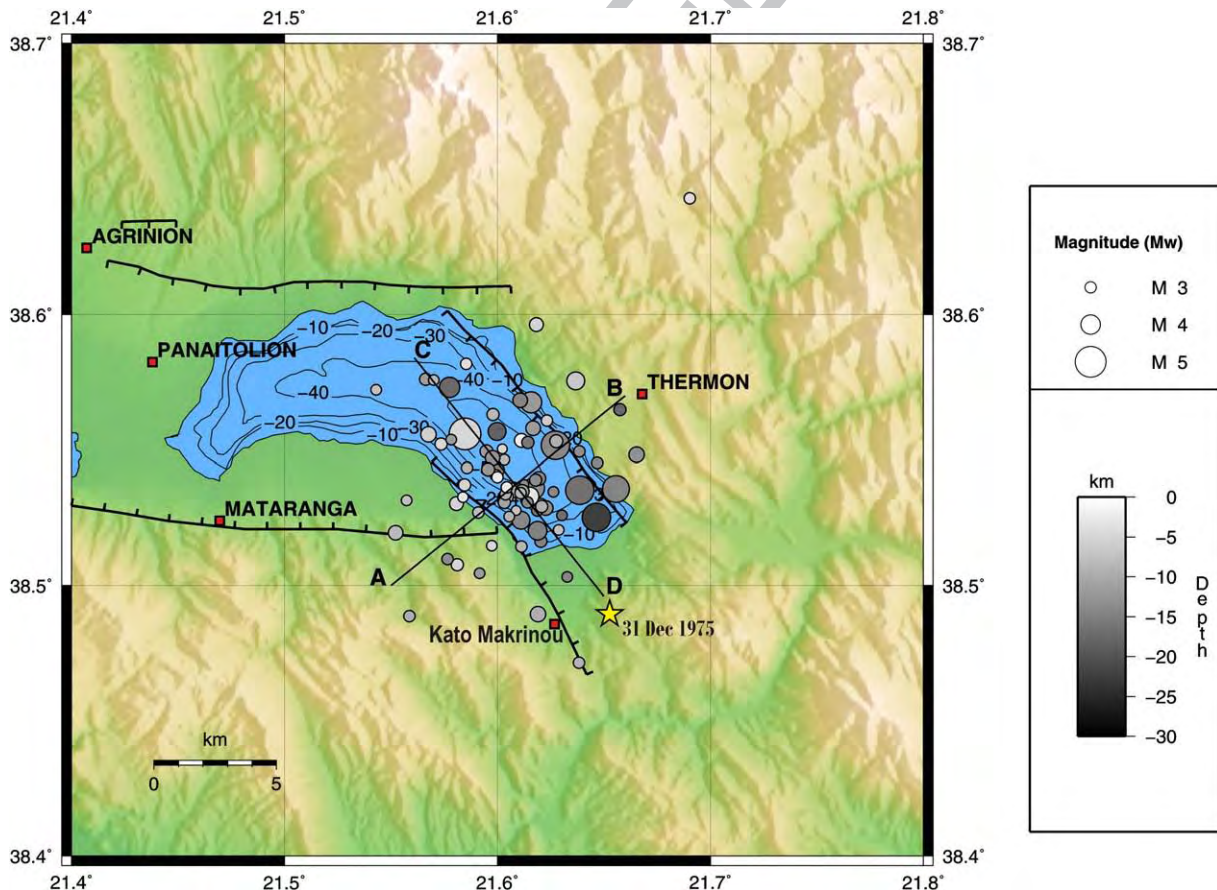


Fig. 6. Distribution of the best located events using Hypoinverse. Earthquake activity is well confined along the two NNW–ESE trending normal faults bounding the eastern banks of Trichonis Lake.

173 fixed, realigning the waveforms if necessary, and inverting for
 174 synthetics. The normal faulting solution deteriorates the amplitude fit
 175 and predicts reversed polarity, compared to the observed, at three
 176 stations (comparison not shown here).

177 3.2. Relocation of the epicentres of the 1975 events – macroseismic 178 observations

179 Both the 30 June and 31 December, 1975 events were relocated
 180 using Hypoinverse, the velocity model of Haslinger et al. (1999) and
 181 the available phases at the International Seismological Centre (ISC).
 182 The best solutions (Table 1) place the epicentres near the village of
 183 Kato Makrinou, where the maximum intensities (I=VII–VIII and I=IX,
 184 respectively) have been reported (ISC – on-line bulletin).

185 From the two nodal planes of the 31 December 1975 event it is not
 186 easy to identify the fault plane. First of all, no aftershock locations are
 187 available and only their origin time is provided (Kourouzidis, 2003).
 188 Thus, we re-examined the distribution of the reported MM intensities
 189 (ISC bulletins and NOA bulletins) for the June–December 1975 strong
 190 events, seeking for evidence for the fault plane. We applied the BOXER
 191 code (Gasperini et al., 1999; Gasperini and Ferrari, 2000) and the
 192 relations of MM to MCS scale (Trifunac and Živčić, 1991) to obtain the
 193 macroseismic epicentre and magnitudes, M_w (Table 1). The moment
 194 magnitudes for the June and December events, thus obtained, are 5.9
 195 and 5.6, respectively. Based on the same intensity data, the physical
 196 dimensions and the orientation of the source (for details see Gasperini
 197 et al., 1999) may also be determined. The results indicate an
 198 orientation of 137° for the causative fault of the 31 December 1975
 199 event, while for the 30 June 1975 event they indicate an orientation of

112°, suggesting a NW–SE orientation of the causative fault for these
 200 events (the sense of dip cannot be determined with this method). 201

The instrument that recorded both the 30 June and 31 December
 202 1975 events was a SR-100 Wilmot ($T=0.75$ s, nominal damping=0.10)
 203 seismoscope located at the town of Messolongi ($38.36^\circ\text{N } 21.45^\circ\text{E}$)
 204 approximately 24 km to the SW of the epicentre (Delibasis and
 205 Carydis, 1977) and the records shown in Fig. 3 are those as included in
 206 the National Observatory of Athens (NOA) monthly bulletins. The 30
 207 June 1975 caused a deflection of 13.6 mm in the $\text{N}120^\circ\text{E}$ direction and
 208 the 31 December 1975 event caused a deflection of 13.5 mm in the
 209 $\sim\text{N}130^\circ\text{E}$ direction (Person, 1977). The reported intensities at
 210 Messolongi are I=IV–V MM for both events. Using the maximum
 211 seismoscope deflections, the characteristics of the Wilmot seismo-
 212 scope and the formulation of Jennings and Kanamori (1979; Eqs. (14)
 213 and (15)) we calculate the corresponding Wood–Anderson amplitude
 214 to be ~ 18.9 m (one-half peak-to-peak) and the resulting ML is of the
 215 order of 5.9 for both events. This is contradictory to the fact that the
 216 first (June) event has teleseismic waveforms indicating a smaller
 217 magnitude compared to the second (December) event, and also to the
 218 fact that the raw intensity data as well as the macroseismic moment
 219 magnitudes additionally indicate different magnitudes. Unfortu-
 220 nately the seismoscope records cannot resolve the fault plane, as both
 221 nodal planes for the December 1975 event predict maximum
 222 displacement in the NNW–SSE direction. 223

Taking into consideration the work of Delibasis and Carydis
 224 (1977), who studied in detail the 1975 sequence, the fault structure,
 225 our analysis of the macroseismic observations, previous (Brooks
 226 et al., 1988; Tselentis, 1998 (especially Fig. 4a)) and recent works
 227 (Vött, 2007) we conclude that the June–December 1975 sequence 228

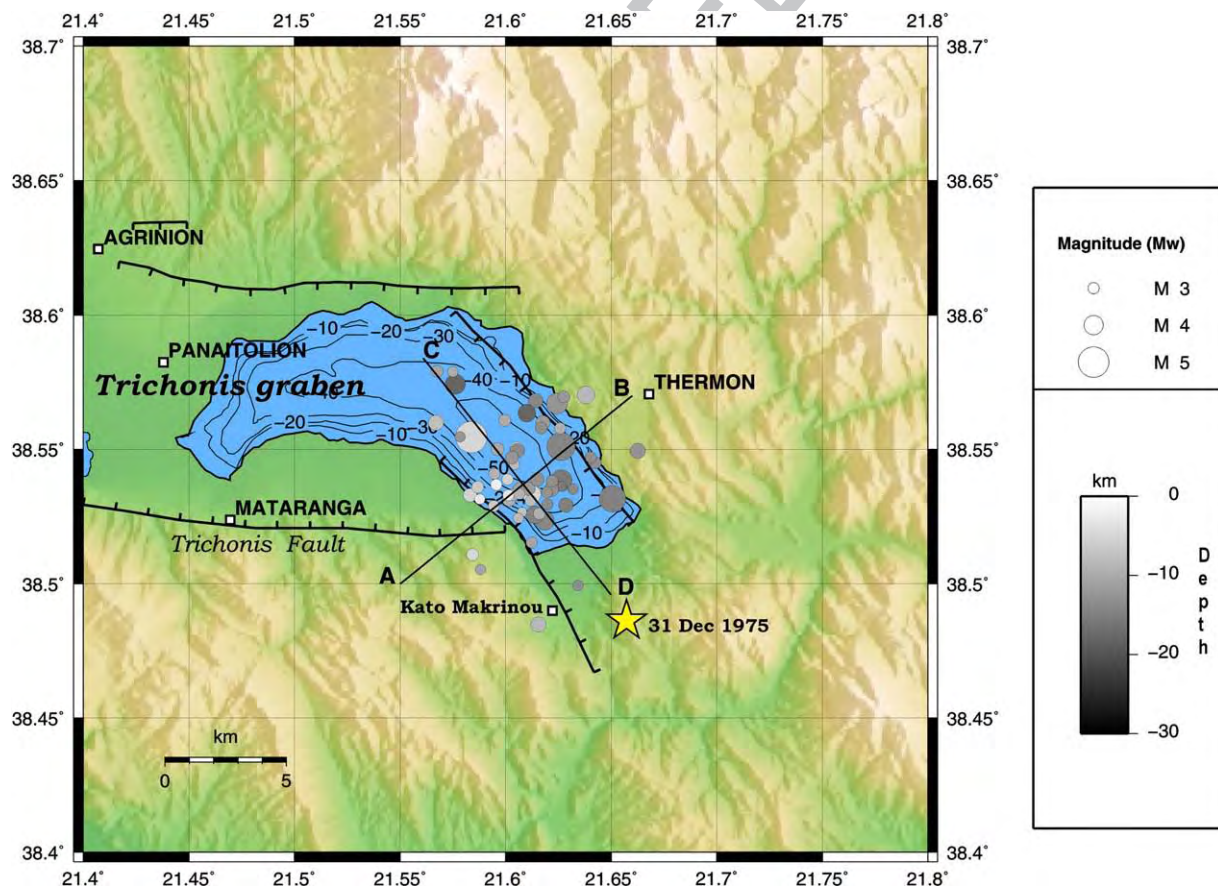


Fig. 7. Our preferred distribution of epicentres using HypoDD and the approach defined in the text. Seismicity is clustering in a NNW–ESE direction, within the eastern part of Lake Trichonis, and is well confined within the two normal faults bounding the banks of the lake. Lines AB and CD define the cross-sections in Fig. 8.

229 was the result of the activation of an NNW–ESE trending normal
230 fault that dips to the NE, with sinistral strike-slip motion. The 2007
231 swarm exhibited the same pattern as shown later.

232 4. The April 2007 swarm

233 4.1. Focal mechanisms of the 2007 swarm

234 We used moment tensor inversion applied to regional broad-band
235 waveforms to determine the focal mechanisms of twenty-three (23)
236 events of the 2007 swarm. The waveforms were retrieved from the
237 broad-band stations of the Hellenic Unified Seismic Network (Fig. 4).
238 The ISOLA code, (Sokos and Zahradnik, in press) was used to invert
239 the data to retrieve the moment tensor. The method is a modification
240 of the Kikuchi and Kanamori (1991) iterative deconvolution method
241 to regional distances and it includes the computation of the full
242 Green's functions using the discrete wavenumber of Bouchon (1981,
243 2003). The method allows for multiple source inversion; however for
244 the moderate magnitude events studied here, single source inversion
245 was used. The velocity model of Haslinger et al. (1999) was employed
246 since it was obtained by tomographic investigations in the studied
247 area. The frequency band for the inversion was variable depending on
248 the magnitude of the events; typical values were 0.03 to 0.08 Hz for
249 the strongest events of the swarm and 0.08–0.14 Hz for the moderate
250 magnitude ones. A typical fit for one event (a B solution) is presented
251 (Fig. 5a). The parameters of the focal mechanisms are included in
252 Table 2.

253 The focal mechanisms of the 2007 swarm (Fig. 5b) indicate normal
254 faulting combined with strike-slip motions, along mainly NNW–SSE
255 trending planes. Only two of the focal mechanisms studied are pure
256 strike-slip. The resulting average mechanism for the 2007 events
257 (using the RAKE software, Louvari and Kiratzi, 1997) has the
258 parameters: Nodal plane 1: strike=325°, dip=52°, rake=-58°; Nodal
259 plane 2: strike=99°, dip=48°, rake=-124°, *T* axis: plunge=2°,
260 trend=N33°E, *P* axis: plunge=65°, trend=N298°E, in accordance
261 with the regional stress field (Kiratzi et al., 1987; Papazachos and
262 Kiratzi, 1996; Papazachos et al., 1998; Kiratzi et al., in press).

263 4.2. Distribution of epicentres of the 2007 swarm

264 We collected all the available phase data (*P*- and *S*-wave arrival
265 times) recently established in the Greece Hellenic Unified Seismic
266 Network (HUSN) and more specifically data from the stations
267 operated by Patras University, Thessaloniki University and the
268 National Observatory of Athens – Geodynamic Institute (Fig. 4)
269 were used, to develop a joint catalogue. From the original data set, we
270 chose only those earthquakes for which 5 or more phases were
271 available. Our final data set consists of 11,798 *P*- and 5831 *S*-wave
272 arrival times, corresponding to 79 earthquakes. In all cases we tried to
273 include *S* arrivals in the closest stations (e.g. SELA, SER, EFP, UPR) to
274 constrain focal depths. For the relocation we used both Hypoinverse
275 (Klein, 2002) and HypoDD (Waldhauser and Ellsworth, 2000) location
276 codes, for reasons of comparison and testing.

277 4.2.1. Hypoinverse relocation

278 During trial initial runs several velocity models as well as starting
279 depths were used and the final solutions which have the lowest rms
280 errors are presented in Fig. 6, corresponding to a starting depth of
281 7 km and the Haslinger et al. (1999) velocity model. In general, we
282 included more than 5 phase readings for each event, and the rms
283 uncertainties ranged from 0.15 to 0.46; mean formal location errors
284 are: rms 0.27 s, ERH 0.71 km and ERZ 2.5 km.

285 The epicentres are confined in the eastern part of Lake Trichonis,
286 within the two NNW–ESE bounding normal faults (Fig. 6). All events
287 are shallow, confined in the upper 20 km of the crust and the number
288 of events gradually decreases with increasing depth.

4.2.2. HypoDD relocation

289 Our preferred locations are based on the HypoDD software
290 following the procedure described in Roumelioti et al. (2003). Initial
291 locations (sources) were taken from the derived catalog while stations
292 located within 200 km from the centroid of the initial epicentral area,
293 were used. Thus, 78 initial sources and 15 stations were evolved in the
294 relocation procedure. The double-difference residuals for the pairs of
295 earthquakes at each station were minimized by weighted least
296 squares using the method of singular value decomposition (SVD).
297

231
232
233
234
235
236
237
238
239
240
241
242
243
244
245
246
247
248
249
250
251
252
253
254
255
256
257
258
259
260
261
262
263
264
265
266
267
268
269
270
271
272
273
274
275
276
277
278
279
280
281
282
283
284
285
286
287
288
289
290
291
292
293
294
295
296
297
298
299
300
301
302
303
304
305
306
307
308
309
310
311
312
313
314
315
316
317
318
319
320
321
322
323
324
325
326
327
328
329
330
331
332
333
334
335
336
337
338
339
340
341
342
343
344
345
346
347
348
349
350
351
352
353
354
355
356
357
358
359
360
361
362
363
364
365
366
367
368
369
370
371
372
373
374
375
376
377
378
379
380
381
382
383
384
385
386
387
388
389
390
391
392
393
394
395
396
397
398
399
400
401
402
403
404
405
406
407
408
409
410
411
412
413
414
415
416
417
418
419
420
421
422
423
424
425
426
427
428
429
430
431
432
433
434
435
436
437
438
439
440
441
442
443
444
445
446
447
448
449
450
451
452
453
454
455
456
457
458
459
460
461
462
463
464
465
466
467
468
469
470
471
472
473
474
475
476
477
478
479
480
481
482
483
484
485
486
487
488
489
490
491
492
493
494
495
496
497
498
499
500
501
502
503
504
505
506
507
508
509
510
511
512
513
514
515
516
517
518
519
520
521
522
523
524
525
526
527
528
529
530
531
532
533
534
535
536
537
538
539
540
541
542
543
544
545
546
547
548
549
550
551
552
553
554
555
556
557
558
559
560
561
562
563
564
565
566
567
568
569
570
571
572
573
574
575
576
577
578
579
580
581
582
583
584
585
586
587
588
589
590
591
592
593
594
595
596
597
598
599
600
601
602
603
604
605
606
607
608
609
610
611
612
613
614
615
616
617
618
619
620
621
622
623
624
625
626
627
628
629
630
631
632
633
634
635
636
637
638
639
640
641
642
643
644
645
646
647
648
649
650
651
652
653
654
655
656
657
658
659
660
661
662
663
664
665
666
667
668
669
670
671
672
673
674
675
676
677
678
679
680
681
682
683
684
685
686
687
688
689
690
691
692
693
694
695
696
697
698
699
700
701
702
703
704
705
706
707
708
709
710
711
712
713
714
715
716
717
718
719
720
721
722
723
724
725
726
727
728
729
730
731
732
733
734
735
736
737
738
739
740
741
742
743
744
745
746
747
748
749
750
751
752
753
754
755
756
757
758
759
760
761
762
763
764
765
766
767
768
769
770
771
772
773
774
775
776
777
778
779
780
781
782
783
784
785
786
787
788
789
790
791
792
793
794
795
796
797
798
799
800
801
802
803
804
805
806
807
808
809
810
811
812
813
814
815
816
817
818
819
820
821
822
823
824
825
826
827
828
829
830
831
832
833
834
835
836
837
838
839
840
841
842
843
844
845
846
847
848
849
850
851
852
853
854
855
856
857
858
859
860
861
862
863
864
865
866
867
868
869
870
871
872
873
874
875
876
877
878
879
880
881
882
883
884
885
886
887
888
889
890
891
892
893
894
895
896
897
898
899
900
901
902
903
904
905
906
907
908
909
910
911
912
913
914
915
916
917
918
919
920
921
922
923
924
925
926
927
928
929
930
931
932
933
934
935
936
937
938
939
940
941
942
943
944
945
946
947
948
949
950
951
952
953
954
955
956
957
958
959
960
961
962
963
964
965
966
967
968
969
970
971
972
973
974
975
976
977
978
979
980
981
982
983
984
985
986
987
988
989
990
991
992
993
994
995
996
997
998
999
1000

Table 3											3.1
Relocated epicentres of the 2007 swarm using HypoDD (see text for details)											3.2
No.	Year	Month	Day	Hour	Minute	Second	Lat °N	Lon °E	Depth (km)	Mw	3.3
1	2007	4	9	23	27	15.77	38.539	21.626	15.66	4.2	3.4
2	2007	4	10	0	6	15.07	38.536	21.626	15.61	2.9	3.5
3	2007	4	10	0	8	52.48	38.540	21.614	13.09	2.7	3.6
4	2007	4	10	0	54	56.42	38.529	21.629	14.91	3.5	3.7
5	2007	4	10	1	48	51.26	38.544	21.604	8.34	2.9	3.8
6	2007	4	10	3	17	56.17	38.551	21.626	14.29	4.8	3.9
7	2007	4	10	3	27	38.4	38.534	21.612	5.28	3.9	3.10
8	2007	4	10	3	32	34.33	38.524	21.619	14.15	3.9	3.11
9	2007	4	10	3	39	19.08	38.549	21.663	12.49	3.6	3.12
10	2007	4	10	3	43	6.72	38.485	21.616	8.48	3.6	3.13
11	2007	4	10	4	16	15.63	38.550	21.605	2.95	3.4	3.14
12	2007	4	10	4	29	58.23	38.535	21.607	10.96	3.5	3.15
13	2007	4	10	4	47	18.1	38.535	21.622	12.94	3.5	3.16
14	2007	4	10	5	20	0.61	38.533	21.583	5.70	3.4	3.17
15	2007	4	10	5	39	8.14	38.558	21.626	9.35	3.1	3.18
16	2007	4	10	5	55	12.3	38.531	21.602	9.70	3.4	3.19
17	2007	4	10	6	3	39.23	38.570	21.638	8.54	3.8	3.20
18	2007	4	10	6	16	8.87	38.536	21.587	6.53	3.2	3.21
19	2007	4	10	6	19	21.07	38.533	21.604	9.39	3.2	3.22
20	2007	4	10	6	32	28.04	38.545	21.643	13.28	3.1	3.23
21	2007	4	10	7	5	44.3	38.539	21.601	5.63	3	3.24
22	2007	4	10	7	13	3.87	38.532	21.651	14.60	4.7	3.25
23	2007	4	10	7	14	12.45	38.567	21.624	12.42	4.2	3.26
24	2007	4	10	7	15	40.62	38.555	21.584	5.06	5.1	3.27
25	2007	4	10	7	33	7.59	38.535	21.611	11.82	3.4	3.28
26	2007	4	10	7	35	26.16	38.560	21.567	7.81	3.6	3.29
27	2007	4	10	7	36	57.06	38.511	21.584	4.91	3.2	3.30
28	2007	4	10	7	47	32.03	38.550	21.596	10.22	3.3	3.31
29	2007	4	10	8	13	45.5	38.526	21.614	14.59	3.8	3.32
30	2007	4	10	8	25	17.1	38.527	21.608	7.44	2.8	3.33
31	2007	4	10	9	31	7.17	38.537	21.596	2.29	3	3.34
32	2007	4	10	9	59	1.57	38.560	21.618	11.63	3.5	3.35
33	2007	4	10	10	34	47.96	38.550	21.606	13.62	3.5	3.36
34	2007	4	10	11	27	23.5	38.547	21.640	13.45	3.1	3.37
35	2007	4	10	11	27	50.7	38.541	21.595	9.03	3	3.38
36	2007	4	10	11	29	1.13	38.515	21.612	10.75	3.1	3.39
37	2007	4	10	11	40	16.89	38.499	21.634	13.15	2.9	3.40
38	2007	4	10	11	51	28.9	38.535	21.632	14.02	2.9	3.41
39	2007	4	10	12	14	4.56	38.531	21.612	8.09	3	3.42
40	2007	4	10	12	40	4.89	38.534	21.607	9.13	3	3.43
41	2007	4	10	12	55	17.83	38.539	21.615	12.91	3.4	3.44
42	2007	4	10	13	30	54.09	38.506	21.588	10.95	2.9	3.45
43	2007	4	10	13	46	57.4	38.568	21.614	14.13	3.5	3.46
44	2007	4	10	13	51	0.94	38.564	21.610	17.81	3.8	3.47
45	2007	4	10	16	0	22.63	38.533	21.601	3.52	3	3.48
46	2007	4	10	17	55	50.37	38.525	21.606	8.30	2.9	3.49
47	2007	4	10	22	59	46.72	38.561	21.600	9.87	3.2	3.50
48	2007	4	10	23	32	14.05	38.529	21.595	6.42	3.1	3.51
49	2007	4	10	23	59	17.22	38.555	21.578	12.45	2.9	3.52
50	2007	4	11	0	56	32.62	38.530	21.620	13.71	3.1	3.53
51	2007	4	11	3	39	36.49	38.558	21.617	13.35	3.2	3.54
52	2007	4	11	6	6	32.38	38.579	21.568	10.82	3.2	3.55
53	2007	4	11	7	45	9.26	38.570	21.628	12.03	3.2	3.56
54	2007	4	11	20	6	1.07	38.538	21.622	12.95	3.2	3.57
55	2007	4	11	20	13	13.65	38.534	21.620	12.65	3.1	3.58
56	2007	4	12	10	32	56.08	38.532	21.588	3.01	2.9	3.59
57	2007	4	12	14	32	49.04	38.547	21.603	12.36	3.3	3.60
58	2007	4	13	12	58	14.56	38.526	21.616	9.38	3.2	3.61
59	2007	4	15	2	16	32.54	38.574	21.576	17.86	4.1	3.62
60	2007	4	15	3							

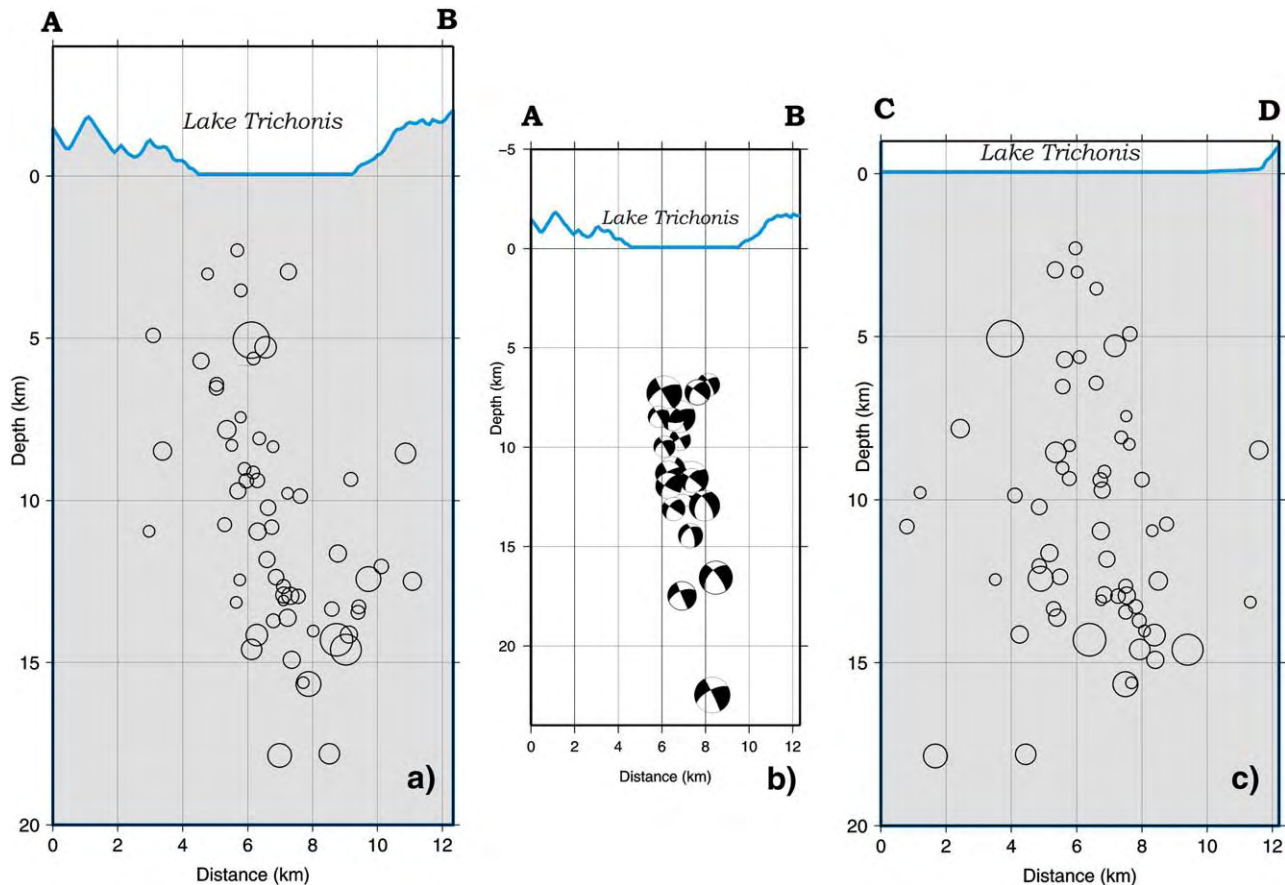


Fig. 8. Cross-sections a) along dip (section AB in Fig. 7) and c) along strike (section CD in Fig. 7) to show the confinement of epicentres within the banks of Lake Trichonis, the dip of the fault plane at $\sim 70^{\circ}$ – 80° to NE, and the depth distribution of the swarm hypocentres to the upper 15 km of the crust. Topography is shown for comparison; b) cross-section along AB and projection of the focal mechanisms to confirm the sense and steepness of dip angles.

Since we were dealing with a small number of events, we selected value 1 for minimum number of observations at each event pair and the number of stations (15) for maximum number of observations at each event pair. The maximum number of neighbouring events was set to the number of the initial sources. Theoretical travel-time differences were estimated based on the 1D P-velocity model (Haslinger et al., 1999) and S-wave velocities were estimated from this model, assuming a V_P/V_S ratio of 1.78 (Kiratzi et al., 1987; Tselentis et al., 1996).

The HypoDD final results include 77% of the sources included in the initial data set (60 relocated events show a spatial pattern more compact compared to previous solutions). The relocated hypocentres (Fig. 7) are clustered mainly at the eastern part of the lake, the centroid of which is defined at Lat: 38.5409° N, Lon: 21.6097° E and at a depth of 10.6 km. The average uncertainties in our locations are: 0.10 km in the E–W direction, 0.05 km in the N–S direction and 0.23 km in the vertical direction, and the rms residual is 8.1 ms. The distribution of epicentres (Table 3 and Fig. 7) is mainly confined within the eastern banks of the lake, reach depths up to 17 km and the strongest events of the swarm are aligned along a NNW–ESE direction, in accordance with the average focal mechanism, previously mentioned, specifically with the nodal plane that strikes at $N325^{\circ}$. The dimensions of this earthquake cluster are approximately $6\text{ km} \times 4\text{ km}$, along strike and along dip, respectively, in accordance with scaling relations for a class M5.2 event (Wells and Coppersmith, 1994).

Fig. 8 presents cross-sections of aftershocks and of focal mechanisms along dip (AB) and along strike (CD) (see also Fig. 7), which indicate: a) steep dip angle of the fault plane ($\sim 70^{\circ}$ – 80°) towards NE, steeper than the dip angle obtained from the 2007 swarm focal

mechanisms, in accordance though with the dip angle (71°) of the 31 Dec 1975 event; b) confinement of earthquake activity in the upper 15 km of the crust and c) evidence for activation of the antithetic fault of the lake, that dips to SW.

5. Stress transfer related to the 1975 event

To model the changes on the stress field after the occurrence of the 31 December 1975 event, using Coulomb stress modelling (Reasenber and Simpson, 1992; Harris and Simpson, 1992), we used the program DLC, written by R. Simpson, based on the subroutines of Okada (1992), assuming elastic rheology (Coulomb failure function or CFF) and static effects. All calculations assumed a Poisson's ratio of 0.25 and a shear modulus of 300,000 bar (30 GPa).

First the stress field due to the Dec 1975 event was calculated using the parameters of Table 1 and assuming a 10 km long and a 8 km wide rupture that satisfies the empirical requirements for a $M_w=6.0$ magnitude earthquake (Wells and Coppersmith, 1994). Then we compute the static stress changes on average fault planes of the 2007 sequence (Fig. 5) i.e. $N325^{\circ}$ E strike, 52° dip to NE and -58° rake. Several runs at various depths in the upper crust were performed and we present here the map of Coulomb stress change for the depth of 10.5 km (Fig. 9), the average depth of the 2007 swarm as shown by the HypoDD procedure (Table 3). Positive stress change (red colours) indicates that slip along receiver faults is encouraged or triggered while negative (blue) change indicates that slip is discouraged or delayed (Fig. 9). We also tested a range of values for the effective coefficient of friction (μ') along the receiver faults and we adopted a value of 0.4 which is considered an average value for regions

Static Coulomb Stress with Uniform Slip

Source Fault 21.661/38.486/6.0/316.0/71.0/10.0000/8.0000/0.374/0.182/-26
At 10.5 km depth on fixed 2007 planes and friction=0.4

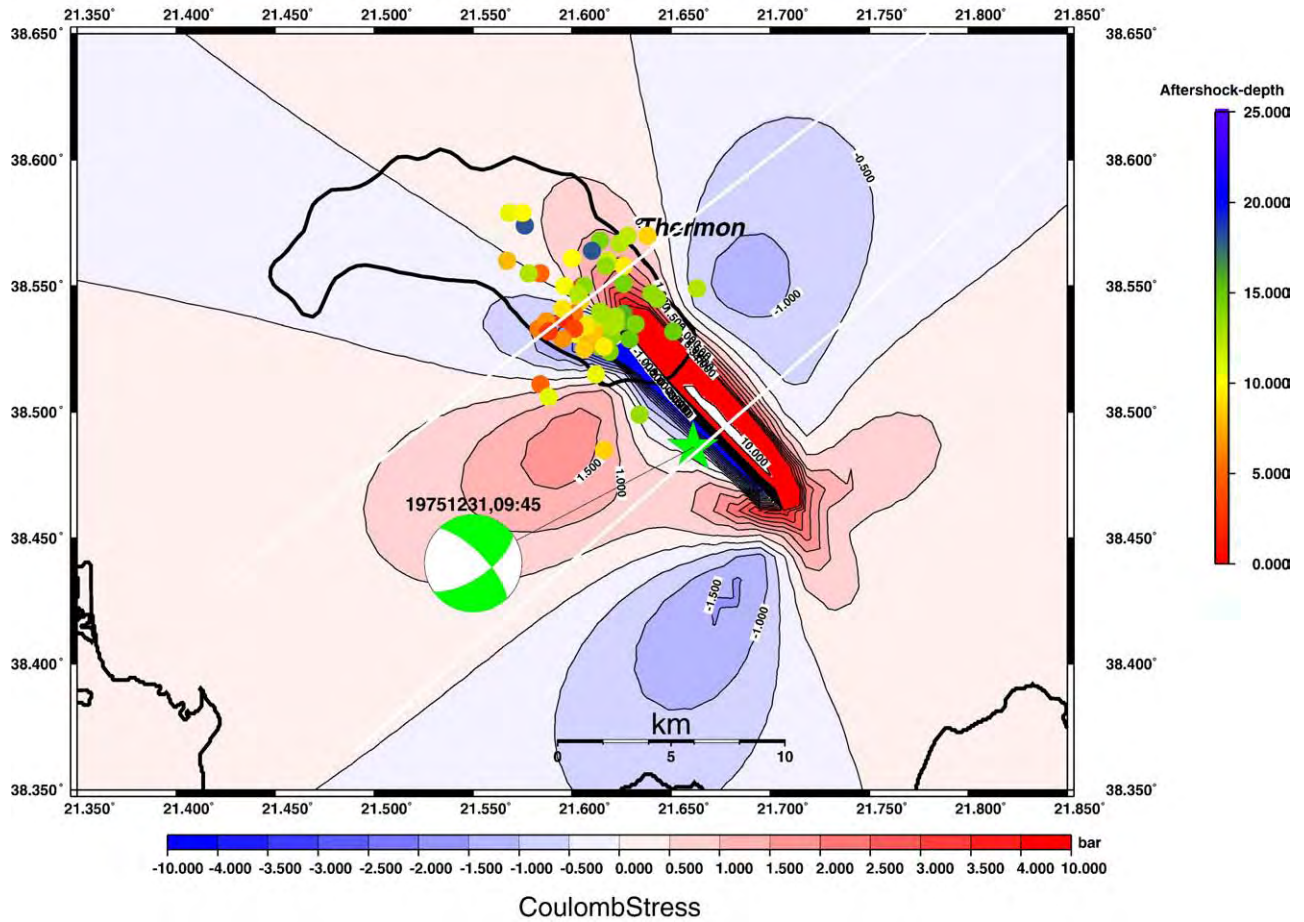


Fig. 9. Map of Coulomb stress changes in the vicinity of the 31 Dec 1975 rupture ($M_w=6.0$). The map shows loaded (red) areas and relaxed (blue) areas at a depth of 10.5 km (average depth of 2007 sequence). Stress calculations are valid for the average slip model of the 2007 sequence (fixed planes). Beach ball indicates focal mechanism of 1975 event and small circles indicate epicentres of the 2007 swarm (colours correspond to different depths). Scale is in bar.

354 containing both mature and minor faults (Parsons et al., 1999). A
355 higher value such as 0.8 gave results with increased levels of Coulomb
356 stress, (ΔCFF) as it is a linear function of the form $\Delta CFF = \Delta \tau + \mu' \Delta \sigma_n$
357 (where $\Delta \tau$ is the change in shear stress resolved along the receiver
358 fault and $\Delta \sigma_n$ is the change in the normal stress acting across the fault
359 plane). As we defined the end of the 1975 rupture at -8 km the
360 Coulomb stress map shows a large load of stress on rocks and fault
361 planes on mid-crust levels (10.5 km; Fig. 9) exceeding 4 bar (0.4 MPa).
362 The 2007 swarm is entirely located to the NW of the 1975 epicentre
363 and outside its rupture plane. We suggest that the majority of the
364 epicentres deeper than 10 km are located in the loaded region and
365 could have been triggered because Coulomb stress levels range from
366 $+0.5$ – 4.1 bar (Fig. 9). In particular, the 20070410, 03:17 event that was
367 third in the sequence with a moment magnitude of 5.0 is located in the
368 loaded region.

369 To investigate the triggering relation graphically we present two
370 cross-sections of ΔCFF in the direction N46E, i.e. normal to the strike of
371 the 1975 rupture plane and also normal to the average strike of the
372 modelled receiver faults (N325°E; Fig. 10). On the same sections one
373 can also see the projections of the April 2007 swarm hypocentres
374 (green dots). The section going through the 1975 hypocentre shows a
375 broad relaxed region exceeding up to 20 km on either side of the
376 rupture and directed NE–SW (Fig. 10a). However, large ΔCFF levels are

observed near the surface (0–3 km) and near the bottom of the fault
377 plane and further down-dip until the depth of 15+ km where they
378 reach 0.5 bar. The post-1975 seismicity (Fig. 1) shows no large
379 earthquakes along NW–SE directed fault planes (or other orientations)
380 so we infer that the stress modelling shown in Fig. 10a is correct. We
381 note that similar stress shadows such as those produced by the 1975
382 events have been observed in the Atalanti region, central Greece, after
383 a double event in April 1894 (Ganas et al., 2006) and their existence
384 influences seismicity rates (Harris and Simpson, 1996). In addition, the
385 NE–SW cross-section at the middle of the 2007 swarm area (Fig. 10b;
386 7 km to the NW of the 1975 epicentre) shows that a broad zone (the
387 red “channel”) of increased ΔCFF has developed with values exceeding
388 4 bar between 5 and 10 km depth. This zone is about 2.5 km wide and
389 dips steeply to the NE. It is located at the NW termination of the 1975
390 rupture. The projection of the 2007 epicentres on this cross-section
391 shows that the majority of the events fall inside this channel of
392 increased ΔCFF . We infer that the occurrence of the 2007 events has
393 been enhanced by stress transfer due to the 1975 mainshock. 394

6. The left-lateral shear north of the Gulf of Corinth 395

The 2007 earthquake swarm together with the processing of the
396 1975 teleseismic data provided new insights into the seismotectonics 397

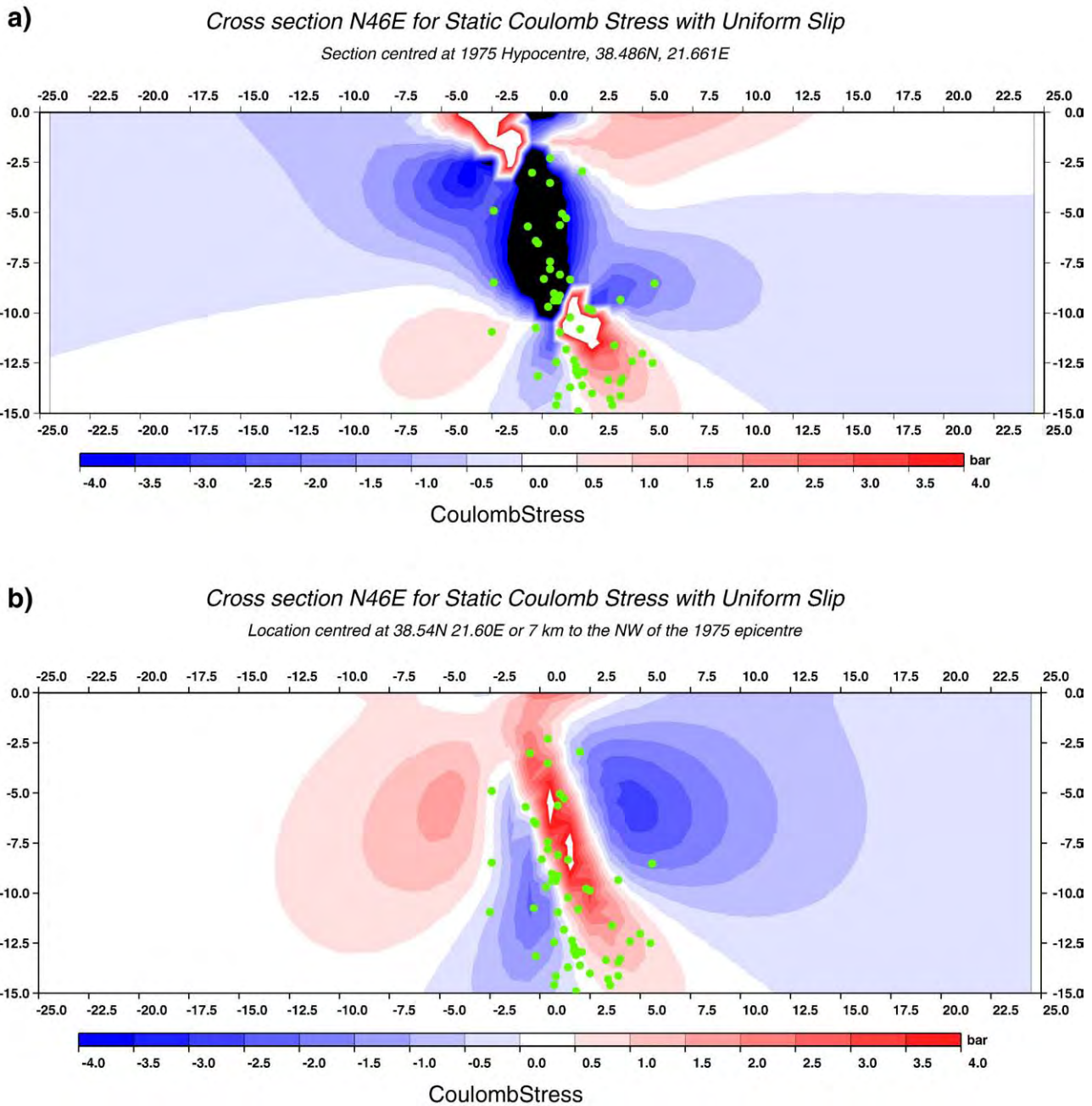


Fig. 10. Vertical cross-sections of Coulomb stress change (ΔCFF) through the upper crust with orientations N46°E (i.e. normal to the 1975 rupture plane); a) section centred at the 1975 hypocentre showing broad relaxation along the rupture plane and stress transfer towards the top and the bottom of the rupture; b) section located 7 km to the NW of the 1975 event (axes in km) showing the stress transfer geometry (high-angle red channel) at the NW termination of the 1975 rupture. Green dots are projected hypocentres of the 2007 swarm. Scale is in bar. Both sections are shown as thin white lines on Fig. 9.

of this region. The new key elements are (Fig. 11): a) the NW–SE strike of the activated fault zone during both the 1975 shallow events and the 2007 swarm b) that those earthquakes did not rupture the Trichonis fault (Fig. 1), which is the most prominent tectonic feature in the region, but they ruptured the NW–SE trending normal fault that bounds the south-eastern bank of the lake and dips to the NE; and c) the left-lateral component of the motion that was mapped throughout the sequence. We suggest that this tectonic setting is due to the activation of a left-lateral, crustal-scale shear zone, about 25 km long. The shear zone links two right-stepping juvenile rifts, the Trichonis and the Corinth graben, respectively (Fig. 11). Ignoring local complexities and minor antithetic faulting the finite extension of the crust in the N–S direction creates a left-lateral simple shear of the upper crust in the tip region

between the two grabens (Fig. 11 inset). Our seismological data are better interpreted by the activation of such a shear zone than some type of “diffuse” deformation between en-echelon rift segments. The southern termination of this left-lateral shear zone may be found in the broader Nafpaktos area (Fig. 11). Indeed, the Nafpaktos area is a relatively low-slip area in comparison to the south coast of the Gulf of Corinth where several north-dipping normal faults are active (Houghton et al., 2003; Palyvos et al., 2005; Bernard et al., 2006).

Our model is developed in Fig. 11 where the long, N–S arrows indicate regional (far-field) extension direction while arrow marked with τ_{max} indicates the resolved shear stress that drives seismic slip along the NW–SE discontinuity. It is possible to drive shear along this fault zone if we assume that locally the stress field has rotated at 45° to

Left-Lateral Shear between right-stepping rifts

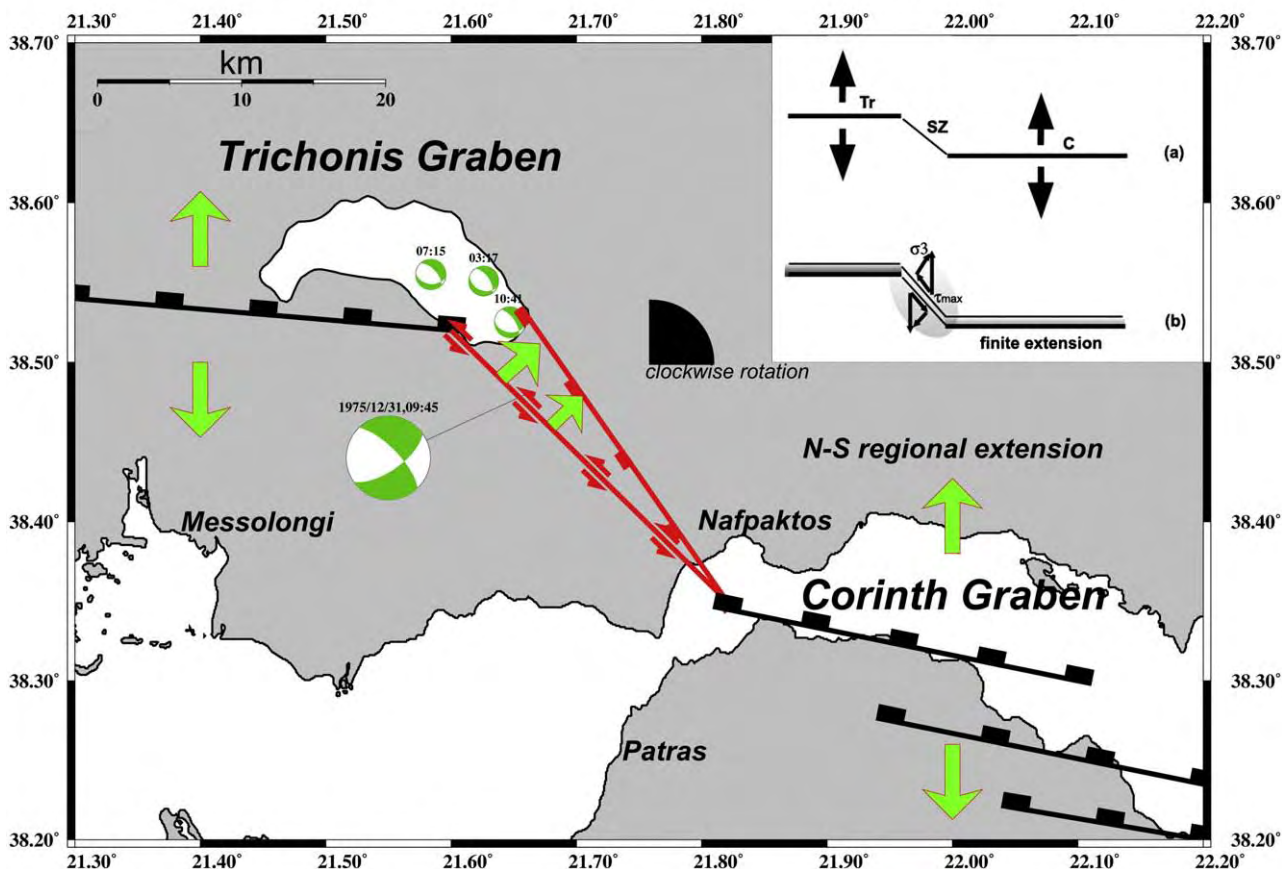


Fig. 11. Map of western Greece showing the structural relationship of the two sub-parallel, E–W striking Quaternary Grabens (Corinth and Trichonis) and the origin of the left-lateral shear along the NW–SE direction between Nafpaktos and Lake Trichonis. Inset sketch shows the development of simple shear deformation between two non-overlapping rifts where σ_3 denotes local minimum compressional stress direction and τ_{\max} plane of maximum shear stress. We propose a 25 km left-lateral shear zone striking NW–SE between the two rifts dipping at a high-angle to the NE. Deformation is dominated by normal faulting because of large, differential rotations of crustal blocks on either side of the Gulf of Corinth that locally create NE–SW extension. Beach balls indicate focal mechanisms of the 31 December 1975 and the three stronger 2007 events (compressional quadrants shaded).

the orientation of the structure (Scholz, 2002, p. 142). We suggest that inside this zone the azimuth of the maximum compressional stress (σ_1) is provided by the orientation of the *P* axis of the earthquakes that we studied (i.e. E–W to SE–NW; Tables 1 and 2). This model is compatible with the N–S directed, far-field extension.

The normal component of the deformation originates from finite strain constraints, i.e. from spreading (new space) that is created due to the clockwise (vertical-axis) rotation of the crustal block to the north of the Gulf of Corinth (Fig. 11; Avallone et al., 2004). The creation of new space is due to the increasing rotation rate from south (2.8° per My) to north (7° per My) as evidenced by the GPS data of Avallone et al. (2004). This “spreading” effect is normal to the trend of the shear zone; however, we note that this local extension is a secondary effect within the prevailing N–S extension since no field evidence exists for a major strike-slip zone in this area, except for the NW–SE orientation of the lake’s coastline near the 2007 swarm epicentres. In the elastic upper crust this spreading is accommodated by slip along normal faults such as the fault that ruptured during the 1975 earthquake and the faults activated during the 2007 swarm. Therefore the model (Fig. 11, inset) includes a small NE–SW arrow marked with σ_3 which indicates the local extension direction as obtained from the average *T*-axis plunge and plunge direction in Table 2 (2/033). This process resembles the extension created at releasing bends of major strike-slip faults known as “pull-apart”, only that in the Trichonis case the releasing factor is the differential clockwise rotation of crustal blocks. As previously mentioned such clockwise rotations are well documen-

ted elsewhere in western Greece from paleomagnetic data (van Hinsbergen et al., 2005, 2006; Vött, 2007). The block rotations are necessary to accommodate large scale deformation of the Hellenic Arc due to a combination of motions from the N215°E-advancing Aegean microplate over the N5°W-moving Nubia plate (Goldsworthy and Jackson, 2002; Fernandes et al., 2003). Another implication of this tectonic model is that the Trichonis graben cannot grow towards the east so the size of future, strong earthquakes along the lake’s south coast can be better constrained.

In summary, our study substantiates the existence of a significant strike-slip component in the active tectonics to the NW of the Gulf of Corinth. Previous studies in this region of western Greece (Hatzfeld et al., 1988; Baker et al., 1997) showed primarily normal or thrust faulting. Hatzfeld et al. (1988) reported two small events with *P* axes trending NW–SE to the east of lake Trichonis but without further discussion. However, strike-slip motions have been recorded inside the Gulf of Patras during the 1993 earthquake sequence ($M_s=5.4$; Tselentis et al., 1994; Tselentis, 1998; Kiratzi and Louvari, 2003) where the NW–SE alignment of aftershocks points to the activation of a left-lateral strike-slip fault. The along-strike extent of the 1993 aftershocks reached 25 km in the NW–SE direction cutting through the eastern part of the Gulf. The Gulf of Patras is a well-studied Quaternary Graben where the main structure is north-dipping (Ferentinos et al., 1985; Chronis et al., 1991). This configuration of active structures resembles closely the Trichonis graben in the sense that both grabens show asymmetry (southern faults are more active) and terminate against NW–SE left-lateral faults.

7. Conclusions

The April 2007 earthquake swarm that occurred in Lake Trichonis provided high quality digital data, to the recently established Hellenic Unified Seismograph Network (HUSN), which we used to relocate epicentres and determine focal mechanisms. The epicentres of 2007 swarm are confined within the eastern shores of the lake – bounded by two NNW–ESE trending normal faults – and in close proximity to the epicentres of the June–December 1975 earthquake sequence, the strongest instrumentally recorded events affecting the region of this study. The majority of those have occurred inside a high-angle “channel” of increased Coulomb stress (Fig. 10) that extends beneath the lake up to mid-crustal levels as a result of the 31 December 1975 earthquake. We applied teleseismic waveform inversion to obtain the focal mechanism of the 31 December 1975 event, and the results show that it was produced by normal faulting along a NNW–ESE striking fault (N316°E), combined with considerable sinistral strike-slip component. The focal mechanisms for 23 events of the 2007 swarm also clearly imply normal faulting along NNW–ESE trending planes, sometimes exhibiting an amount of left-lateral motion.

The 2007 earthquake swarm gave us new insights into the seismotectonics of this region. The new key elements are: a) the NW–SE strike of the activated fault zone, i.e. the 1975 events and the 2007 swarm did not rupture the south Trichonis fault, which is the most prominent tectonic feature in the region, but they ruptured the NW–SE trending normal fault that bounds the south-eastern bank of the lake and dips to the NE; and b) the left-lateral component of the slip vector that was mapped throughout the sequence. We suggest that this tectonic setting is due to the combination of “spreading” due to vertical-axis rotation of crustal blocks and to left-lateral, crustal-scale shear that links two right-stepping normal fault zones, the Trichonis and the Corinth graben, respectively (Fig. 11).

Acknowledgments

We acknowledge (A.K., C.B and Z.R) with thanks financial support from the General Secretariat of Research and Technology (Ministry of Development – Greece), and from INTERREG IIIA. We also thank G. Stavrakakis, the Director of the Geodynamic Institute of Athens, for providing phase data. AG thanks Bob Simpson and Tom Parsons for discussions on stress transfer. Two anonymous reviewers are also thanked for constructive suggestions. Most of the figures were produced using the GMT software (Wessel and Smith, 1998).

References

Ambraseys, N., 2001a. Reassessment of earthquakes, 1900–1999, in the Eastern Mediterranean and the Middle East. *Geophys. J. Int.* 145, 471–485.
 Ambraseys, N., 2001b. Assessment of surface wave magnitudes of earthquakes in Greece. *J. Seismol.* 5, 103–116.
 Avallone, A., Briole, P., Balodimou, A., Billiris, H., Charade, O., Mitsakaki, X., Necessian, A., Papazissi, K., Paradissis, D., Veis, G., 2004. Analysis of eleven years of deformation measured by GPS in the Corinth Rift Laboratory area. *C. R. Geosciences* 336, 301–311.
 Baker, C., Hatzfeld, D., Lyon-Caen, H., Papadimitriou, E., Rigo, A., 1997. Earthquake mechanisms of the Adriatic Sea and Western Greece: implications for the oceanic subduction-continental collision transition. *Geophys. J. Int.* 131, 559–594.
 Benetatos, C., Kiratzi, A., Papazachos, C., Karakaisis, G., 2004. Focal mechanisms of shallow and intermediate depth earthquakes along the Hellenic Arc. *J. Geodyn.* 37, 253–296.
 Benetatos, C., Kiratzi, A., Roumelioti, Z., Stavrakakis, G., Drakatos, G., Latoussakis, I., 2005. The 14 August 2003 Lefkada Island (Greece) earthquake: focal mechanisms of the mainshock and of the aftershock sequence. *J. Seismol.* 9, 171–190.
 Bernard, P.H., Lyon-Caen, P., Briole, A., Deschamps, F., Boudin, K., Makropoulos, P., Papadimitriou, F., Lemeille, G., Patau, H., Billiris, D., Paradissis, K., Papazissi, H., Castarède, O., Charade, A., Necessian, A., Avallone, F., Pacchiani, J., Zahradnik, S., Sacks Linde, A., 2006. Seismicity, deformation and seismic hazard in the western rift of Corinth: new insights from the Corinth Rift Laboratory (CRL). *Tectonophysics* 426, 7–30.
 British Petroleum Co. Ltd, 1971. The geological results of petroleum exploration in western Greece. *Geology of Greece*, vol. 10. IGSR (now IGME), Athens.
 Brooks, M., Ferentinos, G., 1984. Tectonics and sedimentation in the Gulf of Corinth and the Zakynthos and Kefallinia Channels, Western Greece. *Tectonophysics* 101, 25–54.

Brooks, M., Clews, J., Melis, N., 1988. Structural development of Neogene basins in western Greece. *Basin Res.* 1, 129–138.
 Bouchon, M., 1981. A simple method to calculate Green's functions for elastic layered media. *Bull. Seismol. Soc. Am.* 71, 959–971.
 Bouchon, M., 2003. A review of the discrete wavenumber method. *Pure Appl. Geophys.* 160, 445–465.
 Chronis, G., Piper, D., Anagnostou, C., 1991. Late Quaternary evolution of the Gulf of Patras, Greece: tectonism, deltaic sedimentation and sea-level change. *Mar. Geol.* 97 (1–2), 191–209.
 Delibasis, N., Carydis, P., 1977. Recent earthquake activity in Trichonis region and its tectonic significance. *Ann. Geofis.* 30, 19–81.
 Doutsos, T., Kontopoulos, N., Frydas, D., 1987. Neotectonic evolution of northwestern-continental Greece. *Geol. Rundsch.* 76, 433–450.
 Doutsos, T., Kontopoulos, N., Poulimenos, G., 1988. The Corinth–Patras rift as the initial stage of continental fragmentation behind an active island arc (Greece). *Basin Res.* 1, 177–190.
 Ferentinos, G., Brooks, M., Doutsos, T., 1985. Quaternary tectonics in the Gulf of Patras, western Greece. *J. Struct. Geol.* 7, 713–717.
 Fernandes, R., Ambrosius, B., Noomen, R., Bastos, L., Wortel, M., Spakman, W., Govers, R., 2003. The relative motion between Africa and Eurasia as derived from ITRF2000 and GPS data. *Geophys. Res. Lett.* 30, 1828. doi:10.1029/2003GL017089.
 Ganas, A., Sokos, E., Agalos, A., Leontakianakos, G., Pavlides, S., 2006. Coulomb stress triggering of earthquakes along the Atalanti Fault, central Greece: two April 1894 M6+ events and stress change patterns. *Tectonophysics* 420, 357–369.
 Gasperini, P., Ferrari, G., 2000. Deriving numerical estimates from descriptive information: the computation of earthquake parameters. *Ann. Geofis.* 43, 729–746.
 Gasperini, P., Bernardini, F., Valensise, G., Boschi, E., 1999. Defining seismicogenic sources from historical earthquake felt reports. *Bull. Seismol. Soc. Am.* 89, 94–110.
 Goldworthy, M., Jackson, J., Haines, J., 2002. The continuity of active fault systems in Greece. *Geophys. J. Int.* 148, 596–618.
 Harris, R.A., Simpson, R.W., 1992. Changes in static stress on southern California faults after the 1992 Landers earthquake. *Nature* 360, 251–254.
 Harris, R.A., Simpson, R.W., 1996. In the shadow of 1857 – the effect of the great Ft. Tejon earthquake on subsequent earthquakes in southern California. *Geophys. Res. Lett.* 23, 229–232.
 Haslinger, F., Kissling, E., Ansonge, J., Hatzfeld, D., Papadimitriou, E., Karakostas, V., Makropoulos, K., Kahle, H.G., Peter, Y., 1999. 3D crustal structure from local earthquake tomography around the Gulf of Arta (Ionian region, NW Greece). *Tectonophysics* 304, 201–218.
 Hatzfeld, D., Pedotti, G., Hatzidimitriou, P., Makropoulos, K., 1988. The strain pattern in the western Hellenic Arc deduced from a microearthquake survey. *Geophys. J. Int.* 101, 181–202.
 Hatzfeld, D., Kassaras, I., Panagiotopoulos, D.G., Amorese, D., Makropoulos, K., Karakaisis, G.F., Coutant, O., 1995. Microseismicity and strain pattern in North-western Greece. *Tectonics* 14, 773–785.
 Houghton, S.L., Roberts, G.P., Papanikolaou, I.D., McArthur, J.M., Gilmour, M.A., 2003. New ²³⁴U–²³⁰Th coral dates from the western Gulf of Corinth: implications for extensional tectonics. *Geophys. Res. Lett.* 30 (19), 2003. doi:10.1029/2003GL018112.
 Jennings, P.C., Kanamori, H., 1979. Determination of local magnitude ML from 591 seismoscope records. *Bull. Seismol. Soc. Am.* 69, 1267–1288.
 Kokkalas, S., Xypolias, P., Koukouvelas, I., Doutsos, T., 2006. Postcollisional contractional and extensional deformation in the Aegean region. *Geol. Soc. Amer. Bull.* 409, 594–606. Special Paper.
 Kikuchi, M., Kanamori, H., 1991. Inversion of complex body waves—III. *Bull. Seismol. Soc. Am.* 81, 2335–2350.
 Kiratzi, A., Louvari, E., 2003. Focal mechanisms of shallow earthquakes in the Aegean Sea and the surrounding lands determined by waveform modeling: a new database. *J. Geodyn.* 36, 251–274.
 Kiratzi, A., Papadimitriou, E., Papazachos, B., 1987. A microearthquake survey in the Steno dam site in northwestern Greece. *Ann. Geophys.* 592, 161–166.
 Kiratzi, A., Benetatos, C., Roumelioti, Z., in press. Distributed earthquake focal mechanisms in the Aegean Sea. *Bull. Geol. Soc. Greece*, Vol. XXXVII.
 Klein, F.W., 2002. User's guide to HYPOINVERSE-2000, a FORTRAN program to solve earthquake locations and magnitudes. U. S. Geological Survey Open File Report 02-171 Version 1.0.
 Kourouzidis, M.C., 2003. Study of seismic sequences in Greece and its contribution to earthquake prediction. Ph.D. Thesis, Univ. Thessaloniki, 150pp. (in Greek, with an English abstract).
 Lekkas, E., Papanikolaou, D., 1997. Neotectonic Map of Greece, Aitolia-Akarnania sheet (scale 1:100,000). Applied Scientific Program, University of Athens, Dept of Dynamic, Tectonic and Applied Geology, Technical report, 148pp. (In Greek).
 Louvari, E., Kiratzi, A., 1997. Rake: a windows program to plot earthquake focal mechanisms and stress orientation. *Comp. Geosci.* 23, 851–857.
 Melis, N.S., Brooks, M., Pearce, R.G., 1989. A microearthquake study in the Gulf of Patras region, western Greece, and its seismotectonic interpretation. *Geophys. J. Int.* 98, 515–524.
 National Observatory of Athens (NOA), 1975. Monthly bulletins, June–December 1975.
 Okada, Y., 1992. Internal deformation due to shear and tensile faults in a half-space. *Bull. Seismol. Soc. Am.* 82, 1018–1040.
 Palyvos, N., Pantosti, D., De Martini, P.M., Lemeille, F., Sorel, D., Pavlopoulos, K., 2005. The Aigion–Neos Erineos coastal normal fault system (western Corinth Gulf Rift, Greece): geomorphological signature, recent earthquake history, and evolution. *J. Geophys. Res.* 110, B09302. doi:10.1029/2004JB003165.
 Papadopoulos, G.A., Plessa, A., 2000. Magnitude–distance relations for earthquake-induced landslides in Greece. *Eng. Geol.* 58, 377–386.
 Papazachos, B., 1975. Seismic Activity Along the Saronikos–Corinth–Patras Gulfs. National Observatory of Athens, Geodynamic Institute. Monthly Bulletin April 1975, 9 pp.

- 629 Papazachos, C., Kiratzi, A., 1996. A detailed study of the active crustal deformation in the
630 Aegean and surrounding area. *Tectonophysics* 253, 129–154.
- 631 Papazachos, B., Papazachou, C., 2003. *Earthquakes of Greece*, 3rd edition. Ziti
632 Publications, Thessaloniki. 286 pp.
- 633 Papazachos, B., Papaioannou, C., Papazachos, C., Savvaidis, A., 1997. *Atlas of Iseismal*
634 *Maps for Strong Shallow Earthquakes in Greece and Surrounding Area (426 BC–*
635 *1995)*, Publication No. 4. Geophys. Lab., Univ. of Thessaloniki. 176 pp.
- 636 Papazachos, B.C., Papadimitriou, E.E., Kiratzi, A.A., Papazachos, C.B., Louvari, E.K., 1998.
637 Fault plane solutions in the Aegean Sea and the surrounding area and their tectonic
638 implication. *Boll. Geofis. Teor. Appl.* 39, 199–218.
- 639 Parsons, T., Stein, R.S., Simpson, R.W., Reasenber, P.A., 1999. Stress sensitivity of fault
640 seismicity: a comparison between limited-offset oblique and major strike-slip
641 faults. *J. Geophys. Res.* 104, 20183–20202.
- 642 Person, W., 1977. Seismological notes – May–December 1975. *Bull. Seismol. Soc. Am.* 67,
643 1225–1238.
- 644 Reasenber, P.A., Simpson, R., 1992. Response of regional seismicity to the static stress
645 change produced by the Loma Prieta earthquake. *Science* 255, 1687–1690.
- 646 Roumelioti, Z., Kiratzi, A., Melis, N., 2003. Relocation of the July 26, 2001 Skyros Island
647 (Greece) earthquake sequence using the double-difference technique. *Phys. Earth*
648 *Planet Inter.* 138, 231–239.
- 649 Roumelioti, Z., Ganas, A., Sokos, E., Petrou, P., Serpetsidaki, A., Drakatos, G., 2007. Toward
650 a joint catalogue of recent seismicity in western Greece: preliminary results. *Bull.*
651 *Geol. Soc. Greece* 40, 1257–1266.
- 652 Scholz, C., 2002. *The Mechanics of Earthquakes and Faulting*, 2nd ed. Cambridge
653 University Press, Cambridge. 471 pp.
- Q9 654 Sokos, E., Zahradnik, J., in press. ISOLA A Fortran code and a Matlab GUI to perform
655 multiple-point source inversion of seismic data. *Comp. Geosci.*
- 656 Trifunac, M.D., Živčić, M., 1991. A note on instrumental comparison of the Modified
657 Mercalli Intensity (MMI) in the western United States and the Mercalli–Cancani–
658 Sieberg (MCS) intensity in Yugoslavia. *Eur. Earthq. Eng.* 1, 22–26.
- Tselentis, G.-A., 1998. Fault lengths during the Patras 1993 earthquake sequence as
659 estimated from the pulse width of initial P-wave. *Pure Appl. Geophys.* 152, 75–89. 660
- Tselentis, G., Melis, N., Sokos, E., 1994. The Patras (July 14, 1993; Ms=5.4) earthquake
661 sequence. *Bull. Geol. Soc. Greece* 30, 159–165. 662
- Tselentis, G.-A., Melis, N., Sokos, E., Papatsimpa, K., 1996. The Egion June 15, 1995 (6.2 ML)
663 earthquake, Western Greece. *Pure Appl. Geophys.* 147, 83–98. 664
- van Hinsbergen, D.J.J., Langereis, C.G., Meulenkaamp, J.E., 2005. Revision of the timing,
665 magnitude and distribution of Neogene rotations in the western Aegean region. 666
Tectonophysics 396, 1–34. 667
- van Hinsbergen, D.J.J., van der Meer, D.G., Zachariasse, W.J., Meulenkaamp, J.E., 2006.
668 Deformation of western Greece during Neogene clockwise rotation and collision
669 with Apulia. *Int. J. Earth Sci.* 95, 463–490. 670
- Vött, A., 2007. Relative sea level changes and regional tectonic evolution of seven coastal
671 areas in NW Greece since the mid-Holocene. *Quat. Sci. Rev.* 26, 894–919. 672
- Waldhauser, F., Ellsworth, W.L., 2000. A double-difference earthquake location
673 algorithm: method and application to the Northern Hayward fault, California. 674
Bull. Seismol. Soc. Am. 90, 1353–1368. 675
- Wells, D.L., Coppersmith, K.J., 1994. New empirical relationships among magnitude,
676 rupture length, rupture width, rupture area, and surface displacement. *Bull.*
677 *Seismol. Soc. Am.* 84, 974–1002. 678
- Wessel, P., Smith, W.H.F., 1998. New improved version of the Generic Mapping Tools
679 released. *EOS Trans. AGU* 79, 579. 680
- Zacharias, I., Dimitriou, E., Koussouris, T., 2005. Integrated water management scenarios for
681 wetland protection: application to Trichonis Lake. *Environ. Model. Softw.* 20, 177–185. 682
- Zwick, P., McCaffrey, R., Abers, G., 1994. MT5 Program, IASPEI Software Library, p. 4. 683